

Enhancing mechanical and thermal properties of PLLA ligaments with fumed silica nanoparticles and montmorillonite

K. Chrissafis · E. Pavlidou · K. M. Paraskevopoulos ·
T. Beslikas · N. Nianias · D. Bikiaris

Received: 7 June 2010 / Accepted: 8 November 2010 / Published online: 12 December 2010
© Akadémiai Kiadó, Budapest, Hungary 2010

Abstract Nanocomposites of poly(L-lactic acid) (PLLA) containing 2.5 wt% of fumed silica nanoparticles (SiO₂) and organically modified montmorillonite (OMMT) were prepared by solved evaporation method. From SEM micrographs it was observed that both nanoparticles were well dispersed into PLLA matrix. All nanocomposites exhibited higher mechanical properties compared to neat PLLA, except elongation at break, indicating that nanoparticles can act as efficient reinforcing agents. Nanoparticles affect, also, the thermal properties of PLLA and especially the crystallization rate, which in all nanocomposites is faster than that of neat PLLA. From the thermogravimetric curves it can be seen that neat PLLA nanocomposites present a relatively better thermostability than PLLA, and this was also verified from the calculation of activation energy (E). From the variation of E with increasing degree of conversion it was found that PLLA/nanocomposites decomposition takes place with a complex reaction mechanism, with the participation of two different mechanisms. The combination of models, n th order and n th order with autocatalysis (Fn–Cn), for PLLA and PLLA/OMMT as well as the combination of Fn–Fn for

PLLA/SiO₂ give the better results. For the PLLA/OMMT the values of the E for both mechanisms are higher than neat PLLA. For the PLLA/SiO₂ nanocomposite the value of the E is higher than the corresponding value for PLLA, for the first area of mass loss, while the E of the second mechanism has a lower value.

Keywords Poly(lactic acid) · Reinforcement ligaments · Silica nanoparticles · Montmorillonite · Thermal analysis

Introduction

In orthopedic applications the used materials are mainly metallic, ceramic, or polymeric. The main disadvantage of metallic or ceramic is that they are stiffer than natural bones and after a certain time of use they should be removed from the body with a new surgery. In the past few years, biodegradable polymers have been introduced as alternative materials, due to their advantage, compared to the other materials, of being hydrolyzed in fully absorbable products from the organism. Furthermore, their mechanical properties as well as their decomposition rate can be controlled depending on the application. Such biodegradable polymers are poly(glycolic acid), poly(lactic acid), and their copolymers [1, 2]. Primary areas of application include sutures, macroscopic implants for fixation and ligaments. Some disadvantages of these polymers in tissue engineering applications are their poor biocompatibility, release of acidic degradation products, poor processability, and loss of mechanical properties very early during degradation. To improve the properties of polymeric biomaterials, composites and mainly nanocomposites made from synthetic/natural polymers and ceramic nanoparticles may become good alternative materials as scaffolds for growing

K. Chrissafis · E. Pavlidou · K. M. Paraskevopoulos
Solid State Physics Department, School of Physics, Aristotle
University of Thessaloniki, 541 24, Thessaloniki, Macedonia,
Greece

T. Beslikas
2nd Orthopedic Department, Aristotle University
of Thessaloniki, Thessaloniki, Greece

N. Nianias · D. Bikiaris (✉)
Laboratory of Organic Chemical Technology,
Department of Chemistry, Aristotle University of Thessaloniki,
541 24, Thessaloniki, Macedonia, Greece
e-mail: dbic@chem.auth.gr

bone tissue cells, in view of their superior mechanical and bioactive properties compared to conventional materials [3].

Nanotechnology creates materials that potentially outperform, at several boundaries, existing materials in terms of mechanical, electrical, catalytic, and optical properties. Furthermore, from previous studies it was found an increased osteoblast adhesion on polymer casts of nano-sized surface components compared with polymer casts of the conventional fillers [4, 5]. Polymers or other materials as well as polymer nanocomposites may enhance the deposition of calcium phosphate, forming apatite layer on the surface of the implant, also improving protein adsorption and, therefore, improving the adhesion of osteoblasts [6–8]. Consequently, these nanocomposites have attracted extended interest for biomedical applications such as tissue engineering, bone replacement/repair, dental applications, etc.

Of all the promising polyesters in biomedical field, PLLA is the most prevalent since it has good mechanical properties and degrades into nontoxic products. A large number of investigations have been carried out on PLLA and its copolymers, in biomedical applications for resorbable medical implants in the shape of rod, plate, screw, fiber, sheet, sponge, beads for bone, and tissue engineering [9, 10]. Although PLLA-based fracture fixation device has considerably lower tensile modulus than metallic ones and might be inadequate for high load-bearing applications, mechanical properties can be improved by paying attention during fabrication using high modulus fiber reinforcement, hydroxyapatite, or clays to form nanocomposites. Such studies report an increase in the flexural modulus, strength, and moduli values commensurate with bone replacement implants [11, 12]. Fumed silica (SiO_2) has, also, been widely used as a nanofiller for the preparation of polyester/ SiO_2 nanocomposites [13, 14]. It possesses advantages of a light mass, low price, rich resource, high strength and modulus, and good thermal stability. Few studies on PLLA/ SiO_2 nanocomposites have been reported [15–17].

In this study commercial PLLA absorbable reinforcement ligaments for the repair and reinforcement of articulation instabilities, from Cousin Biotech under the trade name Resorbaid[®], have been used to prepare nanocomposites. The Resorbaid flat braids are used for intra- or extra-articular implantation and reinforcement of articular plastic of the knee, the shoulder, or the ankle. The main purpose of this study is to enhance the mechanical and thermal properties of PLLA ligament by using the particular nanoparticles and for this purpose layered silicate clays (montmorillonite) and fumed silica nanoparticles (SiO_2) are chosen. Beyond this, the second task of this study was to evaluate the effect of these nanoparticles on thermal stability of PLLA ligament and to study in details

the kinetics of the thermal decomposition. According to the literature, such a study, concerning the kinetic analysis of thermal decomposition, is limited only in PLLA/OMMT nanocomposites containing 5 wt% clays [18].

Experimental

Materials

Commercially reinforcement ligament consisted of PLLA supplied under the trade name Resorbaid[®] from Cousin Biotech (France). Fumed silica (SiO_2) nanoparticles were supplied by Degussa AG (Hanau, Germany) under the trade name AEROSIL[®] 200, having a specific surface area of $200 \text{ m}^2 \text{ g}^{-1}$ SiO_2 content > 99.8% and average primary particle size 12 nm. Montmorillonite under the trade name Cloisite[®] 20A (OOMMT), which is modified with a dimethyl, dihydrogenated tallow quaternary ammonium chloride salt, was supplied from Southern Clay Products INC., (Gonzales Texas USA). The particle sizes ranged between 2 and 13 μm and have modulus of elasticity 4.657 GPa, tensile strength 101 MPa, and moisture content < 2%. Dichloromethane anhydrous ($\geq 99.8\%$) and tetrahydrofuran anhydrous ($\geq 99.8\%$) were obtained from Aldrich Chemical Co.

Preparation of PLLA nanocomposites

PLLA ligaments were dissolved in a mixture of dichloromethane/tetrahydrofuran 50/50 w/w at room temperature while in the same mixture were dispersed SiO_2 or montmorillonite nanoparticles under sonication for 1 h. The PLLA solution and nanoparticles dispersion were mixed under stirring for 1 h and sonicated for additional 1 h. The mixture remained in room temperature for 24 h for solvent evaporation and dried under vacuum in 110 °C for 24 h. The prepared films were placed in a desiccator to prevent any moisture absorption. Nanocomposites containing 2.5 wt% SiO_2 and 2.5 wt% montmorillonite were prepared with code names PLLA/ SiO_2 and PLLA/OMMT, respectively.

Mechanical properties

Measurements of tensile mechanical properties of the prepared nanocomposites were performed on an Instron 3344 dynamometer, in accordance with ASTM D638, using a crosshead speed of 5 mm/min. Relative thin sheets of about $350 \pm 25 \mu\text{m}$ were prepared using an Otto Weber, Type PW 30 hydraulic press connected with an Omron E5AX Temperature Controller, at a temperature of $190 \pm 5 \text{ }^\circ\text{C}$. The molds were rapidly cooled by immersing them in water at 20 °C. From these sheets, dumbbell-shaped tensile test

specimens (central portions 5×0.5 mm thick, 22 mm gauge length) were cut in a Wallace cutting press and conditioned at 25 °C and 55–60% relative humidity for 48 h. The values of Young's modulus, yield stress, elongation at break, and tensile strength at the break point were determined.

Scanning electron microscopy (SEM)

SEM measurements were carried out using a JEOL JMS-840A scanning microscope equipped with an energy-dispersive X-ray (EDX) Oxford ISIS 300 micro-analytical system. For this purpose fractured surfaces of PLLA nanocomposites in liquid nitrogen were used. All the studied surfaces were coated with carbon black to avoid charging under the electron beam.

Differential scanning calorimetry

Thermal behavior of PLLA and its nanocomposites was studied using a Perkin-Elmer Pyris Diamond differential scanning calorimeter (DSC). The instrument was calibrated with high purity indium and zinc standards. Samples of about 5 mg were used and heated from 20 up to 200 °C with a heating rate 20 °C min⁻¹. At that temperature the samples remained for 5 min, cooled with a cooling rate 300 °C min⁻¹ till 20 °C, and rescanned again. From this scan the melting temperature (T_m), cold crystallization temperature (T_{cc}), and glass transition temperature (T_g) were determined. Crystallization temperature (T_c) from the melt was also recorded by cooling the samples from 200 to 60 °C at a cooling rate of 20 °C min⁻¹.

Thermogravimetric analysis

Thermogravimetric analysis was carried out in a SETARAM SETSYS TG-DTA 16/18 system. Samples (6.0 ± 0.2 mg) were placed in alumina crucibles. An empty alumina crucible was used as reference. PLLA nanocomposites were heated from ambient temperature to 550 °C in a 50 mL min⁻¹ flow of N₂ at heating rates of 5, 10, 15, and 20 °C min⁻¹. Continuous recordings of sample temperature, sample weight, its first derivative, and heat flow were received.

Results and discussion

Microstructure and mechanical properties of PLLA nanocomposites

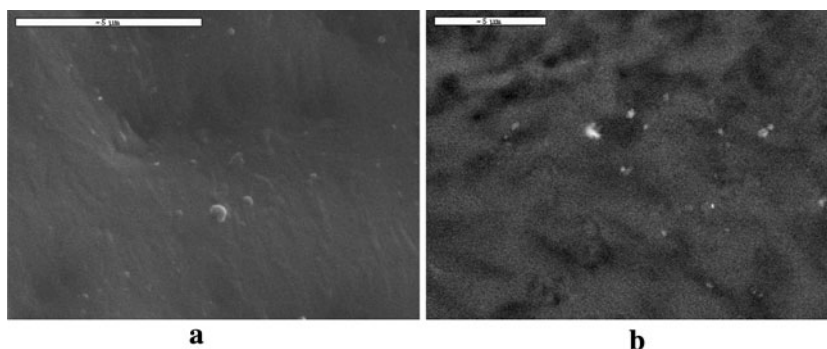
Difficulties arise in dispersing the nanoparticles in polymer matrix due to their strong interactions among themselves,

although the large surface-to-volume ratio makes them with superior properties regarding reinforcement over those with conventional fillers. Due to these inter-nanoparticle interactions; it is extremely difficult to disperse nanoparticles uniformly, especially at higher particle loadings. Several processing methods including shear mixing, mechanical mixing, in situ polymerization, and sonication have been used for dispersing nanoparticles in polymers. The high surface area of nanoparticles attracts the polymer molecule, which reduces the mobility of polymeric chains and, hence, causes increase of viscosity in the polymer matrix. Furthermore, to obtain a uniform dispersion of nanoparticles in the polymer matrix is very difficult due to their insolubility and the inherently poor compatibility between them and polymers. In a previous study [15], in order to enhance the compatibility between PLLA and SiO₂, nanocomposites were prepared into two steps, by grafting L-lactic acid oligomer onto the surface silanol groups of silica nanoparticles followed by melt blending with PLLA. The loading of g-SiO₂ nanoparticles in PLLA matrix greatly improves the toughness and tensile strength of this material. Wu et al. [16] have used a different procedure according to which SiO₂ nanoparticles were well dispersed into PLLA by using acrylic acid grafted polylactide (PLLA-g-AA) as compatibilizer. Tetraethoxysilane used for the preparation of SiO₂ nanoparticles by sol-gel technique is partially compatible with PLLA-g-AA and allows PLLA-g-AA chains to be intercalated into SiO₂ layers. The PLLA-g-AA/SiO₂ hybrid demonstrates dramatic enhancement in thermal and mechanical properties of PLLA. However, in polyesters it is well known that after melting, a reduction of their molecular weight is taking place, which could reduce the mechanical properties of the final material. For these reasons, in this study a solvent evaporation method was used to prepare the nanocomposites. The mixture of dichloromethane/tetrahydrofuran 50/50 w/w was chosen since from preliminary experiments it was found that nanoparticles are well dispersed avoiding precipitation.

As can be seen from Fig. 1a the SiO₂ nanoparticles are well dispersed into PLLA ligament since no aggregates are observed. This good dispersion should be attributed to the interactions between silanol groups of SiO₂ with carbonyl and hydroxyl end groups of PLLA. This increased adhesion may result to enhancement of mechanical properties. Also, a fine dispersion was observed for clay nanoparticles (Fig. 1b). This good dispersion of both nanoparticles throughout the PLLA matrix may lead to a significant enhancement of its mechanical properties.

From stress-strain curves of neat PLLA and its nanocomposites with different nanoparticles it was shown that neat PLLA is a very brittle material, exhibits yielding with a short quasi constant stress regime, and fails at ca. 10%

Fig. 1 SEM micrographs of **a** PLLA/SiO₂ and **b** PLLA/OMMT nanocomposites



strain. The same behavior appears also when OMMT and SiO₂ nanoparticles are added and elongation at break is smaller than in neat PLLA. This is in disagreement with a previous study of Jiang et al. [19] where it was found that elongation at break of PLLA is increased with the incorporation of montmorillonite nanoparticles. However, in our samples a small increase was recorded in tensile strength at break point. Neat PLLA has a tensile strength at break of ca. 58.2 MPa while the corresponding values of PLLA/SiO₂ and PLLA/OMMT nanocomposites are 64.3 and 65.3 MPa, respectively. Increased mechanical properties were also reported from Wen et al. [20] in PLLA/SiO₂ nanocomposites prepared by melt mixing as well as in PLLA/clay nanocomposites [21]. It is obvious that nanoparticles play an important role regarding their efficiency in acting as reinforcement agents. Furthermore, the used treatment with the particular mixture of solvents was appropriate in order to achieve a fine dispersion of nanoparticles into PLLA.

Of primary importance among the mechanical properties of composites is tensile stress at the yield point. As can be seen from Table 1 neat PLLA has a tensile strength at yield point of ca. 63.5 MPa. The corresponding values of PLLA/SiO₂ and PLLA/OMMT nanocomposites containing 2.5 wt% nanoparticles are at 82.6 and 76.3 MPa, respectively. Even though there is a substantial increase in tensile strength at break after nanoparticles incorporation, all the studied nanocomposites can be characterized as brittle materials since they break immediately before yielding. In all nanocomposites, tensile strength at yield point is higher than tensile strength at break. Furthermore, Young's modulus of the studied nanocomposites significantly increased after the addition of nanoparticles. As can be seen from

Table 1, PLLA has a value of 553 MPa while in the case of nanocomposites containing 2.5 wt% of SiO₂ and OMMT the values were increased to 935 and 890 MPa, respectively. These, in combination with the achieved increase of tensile strength at break and yield point, verify that SiO₂ and OMMT nanoparticles incorporation can enhance the mechanical performance of PLLA ligament.

Thermal analysis

Mechanical properties, except reinforcing effect of nanoparticles, could be also affected from the degree of crystallinity of PLLA. It is well known that nanoparticles can also enhance the crystallization rates of semicrystalline polymers. For this reason thermal properties of the prepared nanocomposites were also studied. The melting point of PLLA was recorded at 170.8 °C while in its nanocomposites a slight increase was observed. Thus, the samples containing 2.5 wt% SiO₂ present a melting point at 175 °C while the samples containing OMMT, at 172.8 °C (Fig. 2). This could be attributed to a nucleation effect imposed by the nanoparticles that are increasing the degree of crystallinity of polyesters, or due to the formation of crystals with higher perfection [18]. This can be confirmed, also, from the values of the heat of fusion (Table 2), which in all nanocomposites is higher than the corresponding value of neat PLLA. Thus, the degree of crystallinity (X_c) of nanocomposites—as was calculated based on the enthalpy of fusion of 100% crystalline PLLA, which is 93 J g⁻¹ [22]—is increasing in nanocomposites. Neat PLLA presents a degree of crystallinity 54.4% while after the addition of SiO₂ and OMMT it increased to 59.4 and 56.6%, respectively (Table 2).

Table 1 Mechanical properties of PLLA and its nanocomposites

Sample	Tensile strength at yield/MPa	Tensile strength at break/MPa	Elongation at break/%	Young's modulus/MPa
PLLA	63.5 ± 2.1	58.2 ± 1.5	10 ± 1	553 ± 25
PLLA/SiO ₂	82.6 ± 2.1	64.3 ± 1.2	12 ± 1	935 ± 42
PLLA/OMMT	76.3 ± 1.7	65.3 ± 1.6	2 ± 0.5	890 ± 35

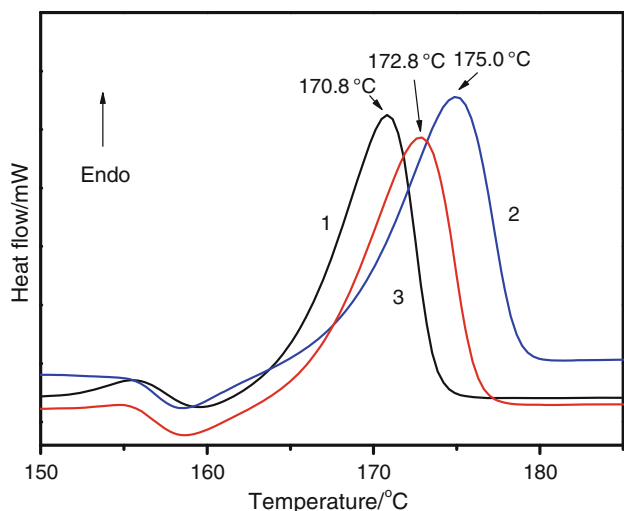


Fig. 2 Melting points of PLLA nanocomposites. 1 PLLA, 2 PLLA/SiO₂, and 3 PLLA/OMMT

Table 2 Thermal properties of PLLA and its nanocomposites

Sample	$T_m/^\circ\text{C}$	$T_g/^\circ\text{C}$	$T_c/^\circ\text{C}$	$T_{cc}/^\circ\text{C}$	$\Delta H_m/\text{J g}^{-1}$	$X_c/\%$
PLLA	170.8	59.2	100.0	103.0	50.6	54.4
PLLA/SiO ₂	175.0	60.5	110.4	98.7	55.2	59.4
PLLA/OMMT	172.8	59.1	105.5	101.6	52.6	56.6

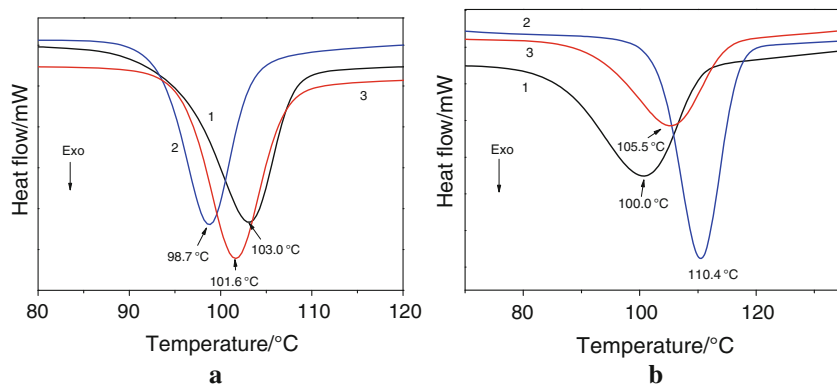
The nucleation effect of SiO₂ and OMMT nanoparticles on PLLA crystallization can be followed more characteristically from the cold crystallization temperature (T_{cc}) measurements. The T_{cc} values of nanocomposites are lower than that of neat PLLA (Fig. 3a). The decrease of T_{cc} means that the cold crystallization of PLLA with nanocomposites becomes easier than in neat PLLA. For example, T_{cc} is decreased from 103.0 °C of neat PLLA to 98.7 °C of PLLA containing SiO₂ and to 101.6 °C of PLLA containing 2.5 wt% OMMT. The lower cold crystallization temperature can be attributed to SiO₂ and OMMT nanoparticles, which acting as nucleating agents

enhance the crystallization of PLLA macromolecules. This is probably due to the fact that nanoparticles have higher surface area in contact with semicrystalline polymer matrices and thus induce a heterogeneous nucleation effect [23, 24]. The concentration dependence of the nucleating effect was also observed in similar compositions of PLLA/clay nanocomposites [25]. A similar trend was, also, found in crystallization temperature from the melt.

As can be seen from Fig. 3b PLLA presents a tiny broad exothermic peak at 100.0 °C. A similar peak is also recorded in the case of PLLA/OMMT nanocomposite but at a higher temperature ca 105.5 °C while in the case of PLLA/SiO₂ nanocomposite, this peak was sharper and appeared at much higher temperature ca. 110.4 °C. These results in combination with T_{cc} values suggested that the incorporation of SiO₂ presents a higher accelerating effect to crystallization rate of PLLA than OMMT nanoparticles.

On the contrary with the above-mentioned shifts, glass transition temperature, T_g , was almost unchanged since only small differences, within 1 °C, were recorded. Usually the T_g of a polymeric matrix tends to increase with the addition of nanoparticles, due to the interactions between the polymer chains and the nanoparticles and also due to the reduction of macromolecular chain mobility at the zone surrounding the nanoparticles [26, 27]. The neat PLLA is characterized by a T_g at 59.2 °C. Similar is the T_g of PLLA/OMMT nanocomposites while the addition of SiO₂ nanoparticles has a small effect on glass transition temperature. The glass transition is a complex phenomenon depending on a number of factors such as chain flexibility, molecular weight, branching, cross-linking, intermolecular interactions, and steric effects. The small increase of T_g after the addition of SiO₂ could be attributed to the decrease in free volume in the polymer matrix due to the physical cross-linkings caused by the interactions taking place between the silanol groups of SiO₂ and PLLA. A similar increase was reported also in PLLA/MWCNTs nanocomposites due to the existence of rigid MWNTs incorporated into the PLLA matrix [28] or in the use of other nanocomposites

Fig. 3 Thermal analysis of PLLA nanocomposites. **a** Cold crystallization temperatures and **b** crystallization temperatures from melt. 1 PLLA, 2 PLLA/SiO₂, and 3 PLLA/OMMT



like clay [29]. However, in our study it seems that the chain segment mobility of the PLLA phase was not influenced by the introduction of SiO₂ or OMMT nanoparticles.

Thermal degradation kinetics

Nanoparticles can also increase the thermal stability of polymers, and this is very important in the case of melt extrusion or injection molding. Therefore, thermal degradation as well as the decomposition mechanism of the prepared nanocomposites were studied by thermogravimetric analysis. The thermogravimetric (TGA) and the derivative thermogravimetric (DTGA) curves of PLLA, PLLA/OMMT, and PLLA/SiO₂ at heating rates 10 °C min⁻¹ are shown in Fig. 4a, b. At ~254 °C PLLA begins to decompose and the decomposition is completed at ~400 °C and its maximum decomposition rate is at 361.6 °C. In PLLA/OMMT nanocomposite the decomposition begins at higher temperature (~264 °C) and is completed at ~415 °C and its maximum decomposition rate is at 365 °C, higher than the same temperature of PLLA [30]. On the contrary, the PLLA/SiO₂ nanocomposite although it begins to decompose at higher temperature (~264 °C) than the PLLA, it completes the decomposition at ~399 °C almost in the same temperature as the PLLA while its maximum decomposition rate is at 349.3 °C, lower enough from the equivalent temperature of PLLA. According to the literature, an improvement in thermal stability was observed for PLLA/SiO₂ nanocomposite containing 2 wt% SiO₂ as compared to that of neat PLLA [31] and also for various concentrations of SiO₂ [16]. The same trend was followed for PLLA/clays (Cloisite® 15A and Cloisite® 30B) nanocomposites [18, 32]. Different results were reported for PLLA/OMMT-Na⁺ [18] and PLLA/C₁₆-OMMT, PLLA/C₁₆-Mica, and PLLA/Cloisite® 25A) indicating that the addition of clays reduces PLLA thermal stability [33]. For these reasons a kinetic study of PLLA thermal decomposition in the presence of SiO₂ nanoparticles and montmorillonite is necessary in order to evaluate the real effect of these nanoparticles.

In order to be analyzed more deeply the degradation mechanisms of PLLA and PLLA/OMMT, PLLA/SiO₂ nanocomposites, it is important that the kinetic parameters (activation energy E and pre-exponential factor A) and conversion function $f(x)$ have to be evaluated. The relationship between kinetic parameters and conversion (α) can be found by using the mass curves recorded in TGA dynamic thermograms. The thermogravimetric (TGA) and the derivative thermogravimetric (DTGA) curves of PLLA/OMMT at different heating rates, 5, 10, 15, and 20 °C min⁻¹, are shown in Fig. 5 as an example of the three different studied polymers. The TGA curves shift to higher temperatures as the heating rate (β) is increased from 5 to 20 °C min⁻¹. The shift of onset to higher temperatures with the increase of β is due to the shorter time required for a sample to reach a given temperature at faster heating rates. This heating rate dependence can also be followed in the DTGA curves. That is, the DTG curves shift toward higher temperatures as the heating rate increases.

For the determination of the activation energy we have chosen to use three different isoconversional methods, comparatively, since every method has its own error. The isoconversional method is in fact a “model free” method [34] which assumes that the conversion function $f(x)$ does not change with the variation of the heating rate for all values of α . It involves the measuring of the temperatures corresponding to fixed values of α by experiments at different heating rates β [35].

First, the Ozawa, Flynn, and Wall (OFW) method [36–38] is used to calculate the activation energy of PLLA, PLLA/OMMT, and PLLA/SiO₂ for different conversion values. The OFW method is based on the equation:

$$\ln \beta = -1.0516 \frac{E}{RT} + \text{const} \quad (1)$$

where E is the activation energy, β is the heating rate, T is the temperature, and R is the gas constant.

Second, Friedman’s method [39] was used. This method is based on the following equation:

Fig. 4 TGA (a) and DTGA (b) curves at heating rate $\beta = 10 \text{ °C min}^{-1}$ of PLLA (1), PLLA/OMMT (2), and PLLA/SiO₂ (3) nanocomposites

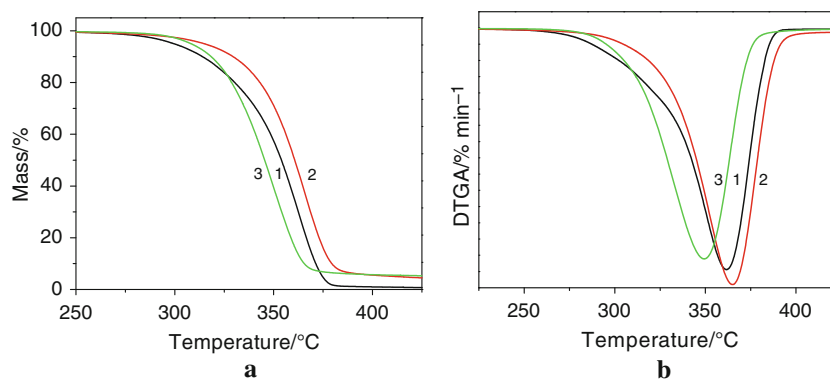
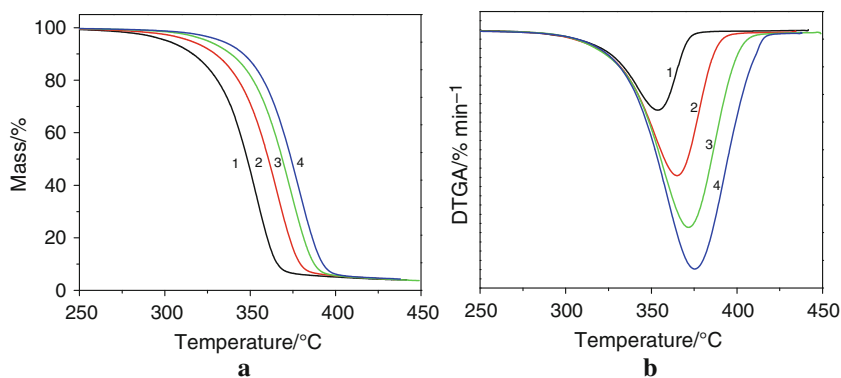


Fig. 5 TGA (a) and DTGA (b) curves of PLLA/OMMT nanocomposite for different heating rates. 1 $\beta = 5 \text{ }^\circ\text{C min}^{-1}$, 2 $\beta = 10 \text{ }^\circ\text{C min}^{-1}$, 3 $\beta = 15 \text{ }^\circ\text{C min}^{-1}$, and 4 $\beta = 20 \text{ }^\circ\text{C min}^{-1}$



$$\ln\left(\beta \frac{d\alpha}{dT}\right) = \ln A + \ln f(\alpha) - \frac{E}{RT} \quad (2)$$

where α is the mass conversion, $f(\alpha)$ is the conversion function (reaction model), and A is the pre-exponential factor.

The calculated values of the activation energy for different values of mass conversion α are shown in Fig. 6. The difference in the E values calculated by the two methods can be explained by a systematic error due to improper integration. The method of Friedman employs instantaneous rate values being, therefore, very sensitive to experimental noise. In Ozawa method the equation used is derived assuming constant activation energy, introducing systematic error in the estimation of E in the case that E varies with α , error that can be estimated by comparison with the Friedman results [40]. It could be followed from Fig. 6, that the dependence of E on α value for PLLA, as calculated with Friedman’s method, can be separated in

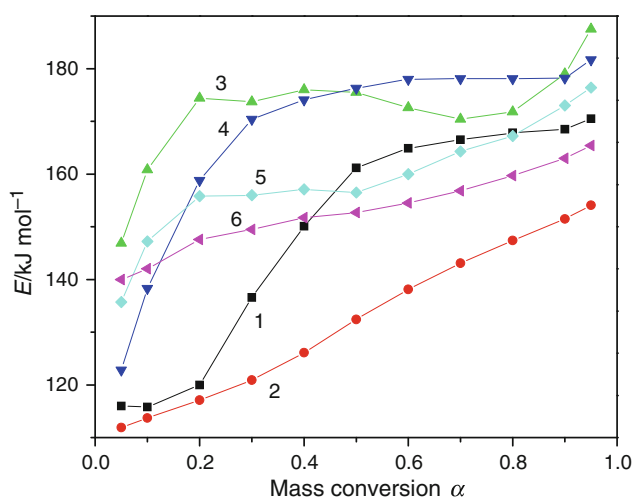


Fig. 6 Activation energy E versus degree of mass conversion α , as calculated according to OFW and Friedman methods. 1 PLLA—Friedman, 2 PLLA-OFW, 3 PLLA/OMMT—Friedman, 4 PLLA/OMMT—OFW, 5 PLLA/SiO₂—Friedman, and 6 PLLA/SiO₂—OFW

three distinct regions, the first for values of α up to 0.2, in which E is almost stable, the second ($0.2 < \alpha < 0.5$), in which E presents a monotonous increase, and the third ($0.5 < \alpha < 0.95$), in which E can be considered as having a constant average value as in the first region. The different regions are not clear in the dependence of E from α as calculated with the OFW method since it presents a monotonous increase. This dependence of E on α is an indication of a complex reaction with the participation of at least two different mechanisms.

For PLLA/OMMT (Fig. 6), the dependence of E on α can be separated in two distinct regions, the first for values of α up to 0.2, in which E presents a monotonous increase and the second ($0.2 < \alpha < 0.95$) in which E can be considered as having a constant average value. Also, for PLLA/SiO₂ (Fig. 6), E presents a monotonous increase for the whole area of mass conversion α . For both nanocomposites this dependence is an indication of a complex degradation reaction. Comparing the mean values of E , as they have been calculated by the two isoconversional methods, it seems that all the E values of PLLA/OMMT are larger than the values of neat PLLA. Also, for the PLLA/SiO₂ only the values of E , for mass conversion lower than 0.4, are larger than the values of PLLA, and for higher mass, conversion values are in the same area. This trend is analogous to the trend of the thermal stability of the three polymers.

According to the third isoconversional method, Kissinger’s method [41],

$$\ln\left(\frac{\beta}{T_p^2}\right) = -\frac{E}{RT_p} + \ln\left(\frac{AR}{E}\right) \quad (3)$$

the activation energy can be calculated by the slope of the linear relationship $\ln(\beta/T_p^2)$ versus $1/T_p$ (Fig. 7) using the inflection point temperatures (T_p). The E values, 142.5, 177.2, and 148.5 kJ mol^{-1} for PLLA, PLLA/OMMT, and PLLA/SiO₂, respectively, are obtained from Kissinger’s curves with regression coefficient better than 0.993. These values indicate that the addition of nanoparticles causes a

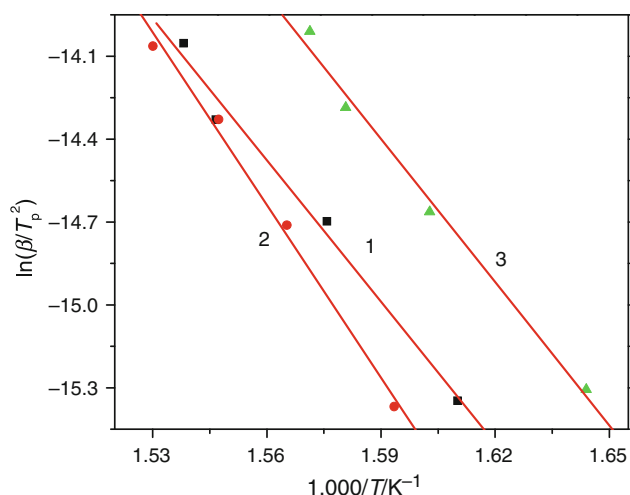


Fig. 7 Kissinger curves of samples PLLA (1), PLLA/OMMT (2), and PLLA/SiO₂ (3)

stabilization effect. Moreover, it is found that the values of E calculated by Kissinger's method coincide with those calculated using the above two methods. The values calculated for the activation energy for PLLA are in the area of the values presented in the literature [18, 42]. As far as we know there is no calculation in the literature for the activation energy of the degradation of the PLLA/SiO₂ but only for PLLA with clays. Zhou et al. [18] studied the PLLA with three different clays, the unmodified montmorillonite-Na⁺, Cloisite[®] 30B, and Cloisite[®] 15A. For the calculation of the activation energy they used the Horowitz–Metzker and Ozawa–Flynn–Wall methods. The average calculated values of E from the two methods presented by them differ a lot, and our values are between them.

The determination of the reaction model using multiple heating rates is based on the “model fitting method” [43] This method involves fitting different models to α -temperature curves and simultaneously determining the activation energy E and the pre-exponential factor A . A variety of 16 well-known kinetic models were used for the fitting, and the conversion range was $0 < \alpha < 1$. In order to determine the nature of the mechanisms through the comparison of the experimental and theoretical data, initially it is considered that the degradation of the samples can be described only by one mechanism, without presuming the exact mechanism. If the result of the fitting cannot be considered as accepted, then we must proceed to the fitting of the experimental data with a combination of two mechanisms. The multivariate nonlinear regression method [43] is used for the determination of the kinetic triplet. The calculated values of E and A after the fitting for three kinetic models (Table 3), for which the quality of the mathematical fitting—depending on the regression coefficient R —is at an accepted level, are presented at Table 4.

Table 3 Three kinetic models and their conversion functions $f(\alpha)$

Kinetic model	Symbol	$f(\alpha)$
n th order	F _n	$(1 - \alpha)^n$
Expanded Prout–Tompkins	B _{na}	$(1 - \alpha)^n \alpha^m$
n th order with autocatalysis	C _n	$(1 - \alpha)^{n(1+K_{cat}\alpha^X)}$

In the studied samples, the best kinetic model is the C_n according to the values of the regression coefficient R . The values of the activation energy for all these models are in the same area with the values that have been calculated with the isoconversional methods. In Fig. 8 the plots of the fitting with the best model C_n for PLLA/OMMT and PLLA/SiO₂ samples are presented. The results of the kinetic study of PLLA have been presented extensively in a previous study [44]. The three kinetic models for the PLLA give the same regression coefficient due to the fact that the variable $\log(K_{cat})$ for the C_n model has negative value, and therefore, the value of K_{cat} is very small and also the value of m for the model B_{na} is very small. So, these two models almost coincide with the model F_n that is mainly used for the degradation of the polymers. For the other two polymers, there are small differences between the values of correlation factors while the difference is more obvious for the F_n model of PLLA/SiO₂.

The quality of the fitting with the C_n model for the three studied samples is good. In PLLA and PLLA/OMMT samples small divergences appear, mainly in the plots with the lower heating rates at the first region, and at the end of the degradation. In PLLA/SiO₂ samples the discrepancies are mainly at the end of the degradation, and the total quality of the fit is better than the fit of the other two polymers.

Knowing that the thermal degradation of the polymers is a very complex reaction, in order to enhance further the quality of the fitting, we must consider more than one reaction mechanisms using the conclusions from the dependence of the activation energy of the partial mass loss.

In the process of identification by two different mechanisms are involved at least six unknown factors. Consequently, the mathematical problem of the identification is very complex and it has several possible solutions. For this reason, at this stage of identification, it is important to limit the scope of the search among all possible combinations of the widely used models. The models that were used and their combinations were only those which have given us satisfactory results from the identification through a single mechanism such as the reaction models F_n, C_n, and B_{na}.

In this stage of identification, for the best possible results we left the parameters (E , A , and n) of the second mechanism to be recalculated and the results are presented

Table 4 Calculated values of E , A of three kinetic models for PLLA, PLLA/OMMT, and PLLA/SiO₂ samples and their regression coefficient R

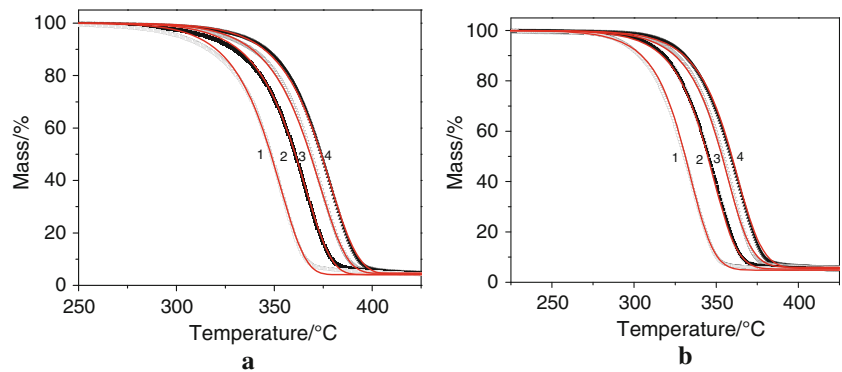
	PLLA			PLLA/OMMT			PLLA/SiO ₂		
	Cn	Bna	Fn	Cn	Bna	Fn	Cn	Bna	Fn
log(A)	8.9	8.9	8.9	11.9	11.8	11.9	10.55	10.85	11.36
E	134.9	135.2	135.3	172.4	169.4	172.4	153.4	153.0	161.2
n	0.42	0.36	0.38	0.9	0.62	0.52	1.07	0.81	0.53
log(K_{cat})	-1.0	2.8E-5 ^a		0.06	7.2E-2 ^a		0.42	0.2 ^a	
R	0.99957	0.99957	0.99957	0.99976	0.99969	0.99967	0.99983	0.99982	0.99958

Conversion range $0 < \alpha < 1$

^a Instead of log(K_{cat})

Fig. 8 TGA curves of PLLA/OMMT (a) and PLLA/SiO₂ (b) nanocomposites and fitting curves with Cn mechanism for different heating rates.

1 $\beta = 5 \text{ }^\circ\text{C min}^{-1}$,
 2 $\beta = 10 \text{ }^\circ\text{C min}^{-1}$,
 3 $\beta = 15 \text{ }^\circ\text{C min}^{-1}$,
 and 4 $\beta = 20 \text{ }^\circ\text{C min}^{-1}$



in Table 5, while the results of the best fitting are presented in Fig. 9 for PLLA/OMMT and PLLA/SiO₂ samples and the fitting to the experimental data is very good for the whole area of mass loss.

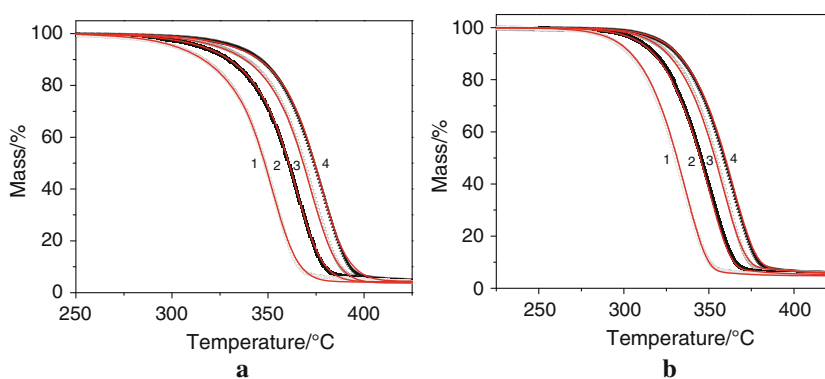
In the Table 5 the results of the best two combinations of models are presented. Since the calculated values of the log(K_{cat}) of the PLLA and PLLA/OMMT have a negative value and, therefore, the parameter K_{cat} is almost zero, the

Cn kinetic model coincides with the Fn model for the first part of mass loss diagram. The values of the activation energy for both mechanisms are in the area of values calculated using the isoconversional methods. In PLLA samples, the mass area calculated in which the first reaction mechanism takes place is 40% and it is in very good agreement with the results of the dependence of the activation energy on the mass conversion α as it has been

Table 5 Activation energy, pre-exponential factor, reaction order, and the regression coefficient of PLLA, PLLA/OMMT, and PLLA/SiO₂ samples after fitting with two reaction mechanisms

First mechanism	PLLA		PLLA/OMMT		PLLA/SiO ₂	
	Cn	Fn	Cn	Fn	Cn	Fn
log(A)	7.6	7.7	10.5	10.5	9.8	10.3
E	116.2	117.3	148.0	148.0	138.6	139.6
n	0.47	0.39	0.48	0.5	1.39	1.58
log(K_{cat})	-0.7		-4.6		0.62	
Second mechanism	PLLA		PLLA/OMMT		PLLA/SiO ₂	
	Cn	Cn	Cn	Cn	Cn	Fn
log(A)	10.8	10.8	12.4	12.4	11.5	11.2
E	161.6	161.3	179.6	179.4	161.7	157.6
n	1.03	1.03	1.31	1.31	0.77	0.61
log(K_{cat})	0.7	0.8	0.66	0.66	-0.33	
R	0.99992	0.99992	0.99988	0.99988	0.99988	0.99988

Fig. 9 TGA curves of PLLA/OMMT (a) and PLLA/SiO₂ (b) nanocomposites and fitting curves with Fn–Cn mechanisms for different heating rates.
 1 $\beta = 5 \text{ }^\circ\text{C min}^{-1}$,
 2 $\beta = 10 \text{ }^\circ\text{C min}^{-1}$,
 3 $\beta = 15 \text{ }^\circ\text{C min}^{-1}$,
 and 4 $\beta = 20 \text{ }^\circ\text{C min}^{-1}$



calculated with the Friedman's method. From this point of view it is obvious why it is better to use more than one method for the calculation of the activation energy. Also, the mass loss area of the first reaction mechanism of the PLLA/OMMT nanocomposite is about 20% and it coincides well with the first area in the dependence of E , as calculated with both Friedman's and OFW methods, of the mass conversion. Comparing the values of the regression coefficient of the best fitting for the PLLA/SiO₂ using one or two reaction mechanisms it can be concluded that, in the case of two reaction mechanisms the improvement of the quality of the fitting was negligible. Although the improvement of the fitting is negligible, the two mechanisms can be accepted in accordance with the slight dependence of E on the mass conversion (Fig. 6) while for the other two materials this dependence is clearer and the two mechanisms must be used. This slight dependence is also accompanied by a combination of two Fn mechanisms which are the simplest models. For the PLLA/OMMT the values of the activation energy for both mechanisms are directly correlated with the conclusions of the thermal stability of this polymer (Fig. 4a,b) in comparison with the PLLA. For the PLLA/SiO₂ nanocomposite the value of the activation energy is larger than the value of E for PLLA, which is in accordance with the better thermal stability of the PLLA/SiO₂ nanocomposite for the first area of mass loss, while the activation energy of the second mechanism has a lower value (Fn–Fn models) than the PLLA.

Conclusions

SiO₂ and OMMT nanoparticles are efficient reinforcing agents for PLLA ligament since by the addition of nanoparticles, tensile strengths at yield point and break as well as Young's modulus were increased. This is very important in the case that PLLA is used as reinforcement ligament.

The nucleation effect of SiO₂ and OMMT nanoparticles on PLLA crystallization can be evaluated through cold crystallization temperature (T_{cc}) measurements. The T_{cc}

values of nanocomposites are lower than that of neat PLLA. Both nanoparticles cause a heterogeneous nucleating effect due to their large available surface area. This has as result all nanocomposites to present higher melting points and degree of crystallinity, compared with neat PLLA.

Also, all nanocomposites present higher thermal stability than that of neat PLLA due to the shielding effect of nanoparticles to the evolution of produced gases during decomposition. The activation energies of PLLA/OMMT are higher than neat PLLA, and for the PLLA/SiO₂ the activation energy for the first area of mass loss is higher and for the second one is somewhat lower. The decomposition of PLLA and PLLA/OMMT can be described accurately by a combination of two consecutive mechanisms (Fn–Cn) taking place in different areas of mass loss and with different activation energies. For the PLLA/SiO₂ one or two mechanisms can be used and for the combination of two mechanisms the simple models of Fn–Fn can be used.

References

- Hayashi T. Biodegradable polymers for biomedical uses. *Prog Polym Sci.* 1994;19:663–702.
- Rezwan K, Chen QZ, Blaker JJ, Boccaccini AR. Biodegradable, bioactive porous polymer/inorganic composite scaffolds for bone tissue engineering. *Biomaterials.* 2006;27:3413–37.
- Balasundaram G, Webster TJ. An overview of nano-polymers for orthopedic applications. *Macromol Biosci.* 2007;7:635–42.
- Boccaccini AR, Gerhardt LS, Rebeling S, Blaker JJ. Fabrication, characterization and assessment of bioactivity of poly(D/L-lactic acid) (PDLLA)/TiO₂ nanocomposite films. *Compos A.* 2005;36:721–7.
- Abarrategi A, Gutierrez M, Moreno-Vicente C, Hortiguala MJ, Ramos V, Lopez-Lacomba JL, Ferrer M, Del Monte F. Multiwall carbon nanotube scaffold for tissue engineering purposes. *Biomaterials.* 2008;29:94–102.
- Kotela I, Podporska J, Soltysiak E, Konsztowicz KJ, Blazewicz M. Polymer nanocomposites for bone tissue substitutes. *Ceram Int.* 2009;35:2475–80.
- Agrawal M, Ray RB. Biodegradable polymeric scaffolds for musculoskeletal tissue engineering. *J Biomed Mater Res.* 2001; 55:141–50.

8. Wei G, Ma PX. Structure and properties of nano-hydroxyapatite/polymer composite scaffolds for bone tissue engineering. *Biomaterials*. 2004;25:4749–57.
9. Satyanarayana D, Chatterji PR. Biodegradable polymers: challenges and strategies. *J Macromol Sci Rev Macromol Chem Phys*. 1993;C33:39–368.
10. Cheung HY, Lau KT, Lu TP, Hui D. A critical review on polymer-based bio-engineered materials for scaffold development. *Compos B Eng*. 2007;38:291–300.
11. Bleach NC, Nazhat SN, Tanner KE, Kellomäki M, Törmälä P. Effect of filler content on mechanical and dynamic mechanical properties of particulate biphasic calcium phosphate—poly(lactide) composites. *Biomaterials*. 2002;23:1579–85.
12. Alexander H, Langrana N, Massengill J, Weiss A. Development of new methods for phalangeal fracture fixation. *J Biomech*. 1981;14:377–87.
13. Vassiliou A, Papageorgiou GZ, Achilias DS, Bikiaris DN. Non-isothermal crystallization kinetics of in situ prepared poly(ϵ -caprolactone)/surface-treated SiO₂ nanocomposites. *Macromol Chem Phys*. 2007;21:364–76.
14. Vassiliou A, Chrissafis K, Bikiaris DN. In situ prepared PBSu/SiO₂ nanocomposites. Study of thermal degradation mechanism. *Thermochim Acta*. 2009;495:120–8.
15. Yan S, Yin J, Yang Y, Dai Z, Ma J, Chen X. Surface-grafted silica linked with L-lactic acid oligomer: a novel nanofiller to improve the performance of biodegradable poly(L-lactide). *Polymer*. 2007;48:1688–94.
16. Wu CS, Liao HT. Modification of biodegradable polylactide by silica and wood flour through a sol-gel process. *J Appl Polym Sci*. 2008;109:2128–38.
17. Wu L, Cao D, Huang Y, Li B. Poly(L-lactic acid)/SiO₂ nanocomposites via in situ melt polycondensation of L-lactic acid in the presence of acidic silica sol: preparation and characterization. *Polymer*. 2008;49:742–9.
18. Zhou Q, Xanthos M. Nanosize and microsize clay effects on the kinetics of the thermal degradation of polylactides. *Polym Degrad Stab*. 2009;94:327–38.
19. Jiang L, Zhang J, Wolcott MP. Comparison of polylactide/nanosized calcium carbonate and polylactide/montmorillonite composites: reinforcing effects and toughening mechanisms. *Polymer*. 2007;48:7632–44.
20. Wen X, Lin Y, Han C, Zhang K, Ran X, Li Y, Dong L. Thermomechanical and optical properties of biodegradable poly(L-lactide)/silica nanocomposites by melt compounding. *J Appl Polym Sci*. 2009;114:3379–86.
21. Chang JH, An YA, Sur GS. Poly(lactic acid) nanocomposites with various organoclays. I. Thermomechanical properties, morphology, and gas permeability. *J Polym Sci B Polym Phys*. 2003;41:94–103.
22. Migliaresi CD, Cohn D, De Lollis A, Fambri L. Dynamic mechanical and calorimetric analysis of compression-molded PLLA of different molecular weights. Effect of thermal treatments. *J Appl Polym Sci*. 1991;43:83–95.
23. Gopakumar TG, Lee JA, Kontopoulou M, Parent JS. Influence of clay exfoliation on the physical properties of montmorillonite/polyethylene composites. *Polymer*. 2002;43:5483–91.
24. Antoniadis G, Paraskevopoulos KM, Bikiaris D, Chrissafis K. Kinetics study of cold-crystallization of poly(ethylene terephthalate) nanocomposites with multi-walled carbon nanotubes. *Thermochim Acta*. 2009;493:68–75.
25. Di YW, Iannace S, Di ME, Nicolais L. Poly(lactic acid)/organoclay nanocomposites: thermal, rheological properties and foam processing. *J Polym Sci B Polym Phys*. 2005;43:689–98.
26. Chrissafis K, Paraskevopoulos KM, Papageorgiou GZ, Bikiaris DN. Thermal and dynamic mechanical behavior of bionanocomposites: fumed silica nanoparticles dispersed in poly(vinyl pyrrolidone), chitosan, and poly(vinyl alcohol). *J Appl Polym Sci*. 2008;110:1739–49.
27. Chen K, Wilkie CA, Vyazovkin S. Nanoconfinement revealed in degradation and relaxation studies of two structurally different polystyrene-clay systems. *J Phys Chem B*. 2007;111:12685–12692.
28. Yoon JT, Jeong YG, Lee SC, Min BG. Influences of poly(lactic acid)-grafted carbon nanotube on thermal, mechanical, and electrical properties of poly(lactic acid). *Polym Adv Technol*. 2009;20:631–8.
29. Krishnamachari P, Zhang J, Lou J, Yan J, Uitenham L. Biodegradable poly(lactic acid)/clay nanocomposites by melt intercalation: a study of morphological, thermal, and mechanical properties. *Int J Polym Anal Charact*. 2009;14:336–50.
30. Chow WS, Lok SK. Thermal properties of poly(lactic acid)/organo-montmorillonite nanocomposites. *J Therm Anal Calorim*. 2009;95:627–32.
31. Zhang J, Lou J, Ilias S, Krishnamachari P, Yan J. Thermal properties of poly(lactic acid) fumed silica nanocomposites: experiments and molecular dynamics simulations. *Polymer*. 2008;49:2381–6.
32. McLauchlin AR, Thomas NL. Preparation and thermal characterization of poly(lactic acid) nanocomposites prepared from organoclays based on an amphoteric surfactant. *Polym Degrad Stab*. 2009;94:868–72.
33. Chang JH, An YU, Cho D, Giannelis EP. Poly(lactic acid) nanocomposites: comparison of their properties with montmorillonite and synthetic mica. *Polymer*. 2003;44:3715–20.
34. Vyazovkin S. Model-free kinetics. Staying free of multiplying entities without necessity. *J Therm Anal Calorim*. 2007;83:45–51.
35. Starink MJ. On the applicability of isoconversion methods for obtaining the activation energy of reactions within a temperature-dependent equilibrium state. *J Mater Sci*. 1997;32:6505–12.
36. Ozawa T. A new method of analyzing thermogravimetric data. *Bull Chem Soc Jpn*. 1965;38:1881–6.
37. Flynn JH, Wall LA. General treatment of the thermogravimetry of polymers. *J Res Natl Bur Stand Phys Chem*. 1966;70A:487–523.
38. Flynn JH, Wall LA. A quick, direct method for the determination of activation energy from thermogravimetric data. *Polym Lett*. 1966;4:323–8.
39. Friedman HL. Kinetics of thermal degradation of char-forming plastics from thermogravimetry. Application to a phenolic plastic. *J Polym Sci C*. 1964;6:183–95.
40. Vyazovkin S. Modification of the integral isoconversional method to account for variation in the activation energy. *J Comput Chem*. 2001;22:178–83.
41. Kissinger HE. Reaction kinetics in differential thermal analysis. *Anal Chem*. 1957;29:1702–8.
42. Zou H, Yi C, Wang L, Liu H, Xu W. Thermal degradation of poly(lactic acid) measured by thermogravimetry coupled to Fourier transform infrared spectroscopy. *J Therm Anal Calorim*. 2009;97:929–35.
43. Opfermann J. Kinetic analysis using multivariate non-linear regression i. Basic concepts. *J Therm Anal Calorim*. 2000;60:641–58.
44. Chrissafis K, Paraskevopoulos KM, Jannakoudakis A, Beslikas T, Bikiaris D. Oxidized multi-walled carbon nanotubes as effective reinforcement and thermal stability agents of PLLA ligaments. *J Appl Polym Sci*. 2010;118:2712–21.